Journal of Engineering Science and Technology
Vol. 21, No. 2 (2026) 495 - 511

INFLUENCE OF SOLVENT AND NON-SOLVENT FABRICATION TECHNIQUES ON THE PROPERTIES OF CCTO-PDMS COMPOSITES

ROSLIN ATHIRAH ROSLAN[1], NURUL HAZLINA NOORDIN[1,2,*], NURULFADZILAH HASAN[1], NOOR ZIRWARTUL AHLAM BINTI NAHARUDDIN[1], NOR HADZFIZAH MOHD RADI[1]

[1]Faculty of Electrical and Electronic Engineering Technology, Universiti Malaysia Pahang Al-Sultan Abdullah (UMPSA)
[2]UMPSA STEM Lab, Faculty of Electrical and Electronic Engineering Technology, Universiti Malaysia Pahang Al-Sultan Abdullah (UMPSA)
*Corresponding author: Nurul Hazlina Noordin hazlina@umpsa.edu.my

Abstract

This study presents a comparative evaluation of calcium copper titanate (CCTO)–polydimethylsiloxane (PDMS) composites fabricated via solvent and nonsolvent techniques, focusing on their morphological, chemical, and dielectric properties relevant to high-frequency microsystem applications. Composites containing 10–60 wt.% CCTO were prepared using ethanol-assisted dispersion (solvent method) and direct blending (nonsolvent method). Morphological and elemental analyses via scanning electron microscopy (SEM) and energy-dispersive X-ray spectroscopy (EDX) revealed improved filler packing and reduced aggregation in nonsolvent-processed samples. Fourier-transform infrared spectroscopy (FTIR) confirmed physical filler–matrix interactions without evidence of chemical bonding. Broadband dielectric measurements across 1–10 GHz showed that nonsolvent composites consistently exhibited higher permittivity and lower dielectric losses. At 60 wt.% loading, the nonsolvent sample demonstrated a dielectric constant of 5.49 and a loss tangent of 0.0417 at 5.2 GHz, alongside an electrical conductivity of 0.066 S/m. These results suggest that solvent-free fabrication enhances dielectric performance while simplifying processing, providing a practical approach for designing flexible substrates for RF and microsystem integration.

Keywords: Composite materials, Flexible antenna, Microstrip patch antenna, Solvent.

1. Introduction

The advancement of flexible electronics has driven the need for dielectric materials with high performance and mechanical compliance, particularly for integration into antennas, sensors, energy storage devices, and wearable systems [1-5]. Flexible electronics are expected to revolutionize consumer electronics, medical devices, and aerospace applications by providing lightweight, durable, and adaptable solutions [2]. One of the primary challenges in developing flexible dielectric materials is achieving a balance between flexibility and high dielectric performance. However, developing materials that combine high dielectric performance with mechanical flexibility remains a persistent challenge in the field of flexible electronics.

Ceramic materials such as $CaCu_3Ti_4O_{12}$ (CCTO) are known for their exceptionally high dielectric constants but are brittle and lack flexibility [6, 7]. In contrast, flexible polymers such as polydimethylsiloxane (PDMS) provide excellent elasticity, transparency, and chemical resistance but have inherently low dielectric constants, which limits their effectiveness in high-frequency or miniaturized electronic systems [8, 9].The challenge, therefore, lies in combining the advantages of both ceramic and polymer systems within a single composite. One of the primary challenges in developing flexible dielectric materials is achieving a balance between flexibility and high dielectric performance.

To overcome these limitations, recent studies have explored composites that combine the flexibility of polymers with the high dielectric properties of ceramics. PDMS/CCTO composites are promising solutions because they leverage the flexibility of PDMS and the high dielectric constant of CCTO. By incorporating CCTO particles into the PDMS matrix, CTO-PDMS composites offer a promising route to achieve this synergy. Previous studies have demonstrated that the dielectric constant of PDMS can be significantly enhanced through the inclusion of CCTO, while maintaining its mechanical elasticity [10-16]. Nevertheless, the performance of such composites is strongly dependent on how the CCTO particles are dispersed and bonded within the PDMS matrix.

Despite this potential, achieving uniform dispersion and strong interfacial bonding between a calcium copper titanate (CCTO) filler and a polydimethylsiloxane (PDMS) matrix remains one of the key challenges in the fabrication of high-performance dielectric composites. Poor filler dispersion can lead to agglomeration, resulting in stress concentrations, premature mechanical failure, and inconsistent dielectric behaviour. The interfacial adhesion between the filler and matrix is equally important, as it governs mechanical reinforcement, load transfer, and dielectric stability. Fabrication techniques play a crucial role in addressing these issues. Hence, improving both particle dispersion and filler-matrix adhesion is crucial for achieving composites with stable dielectric and mechanical behavior.

Solvent-based methods, which typically involve dissolving CCTO in a solvent to facilitate mixing with PDMS, can enhance dispersion but raise concerns over solvent removal, toxicity, and environmental impact. However, solvent-based routes are also associated with drawbacks such as incomplete solvent evaporation, phase separation, and filler re-agglomeration during curing, which can degrade dielectric uniformity and mechanical stability [17, 18].

In contrast, nonsolvent or direct-mixing approaches eliminate solvent-related residues and environmental concerns, providing a cleaner and potentially more reproducible route for flexible substrate fabrication. Nevertheless, achieving homogeneous filler dispersion in nonsolvent systems can be more challenging without strong interfacial control.

Studies have shown that surface modifications of CCTO particles and the use of coupling agents can significantly improve bonding and dielectric properties [10, 19, 20]. Furthermore, processing parameters such as temperature, mixing duration, and shear conditions also influence the final composite quality [21]. Therefore, selecting an appropriate fabrication approach, along with careful control of the interface and process conditions, is critical for optimizing both the electrical and mechanical performance of CCTO-PDMS composites.

While both solvent and nonsolvent techniques are widely utilized in composite fabrication, few studies have systematically compared their effects on morphological, chemical, and electrical properties. Most existing studies tend to investigate either solvent or nonsolvent approaches in isolation, often emphasizing specific outcomes such as dielectric performance, chemical compatibility, or morphological features. For example, solvent-based studies typically focus on how different solvents influence filler dispersion and the dielectric response without extending the analysis to microstructural or chemical characteristics [22, 23].

On the other hand, research involving nonsolvent-based methods, such as nonsolvent-induced phase separation (NIPS), has largely concentrated on processing efficiency, membrane formation, or mechanical properties, with limited attention given to dielectric or interfacial behaviour [24]. Despite these advances, there remains no direct, one-to-one comparison of solvent and nonsolvent processing routes under identical material compositions and characterization conditions. This absence of comparative work creates a gap in understanding how processing methods govern the morphology, interfacial chemistry, and dielectric response of CCTO-PDMS composites.

Therefore, this study aims to systematically compare solvent and nonsolvent fabrication techniques for CCTO-PDMS composites to clarify how processing route affects filler distribution, chemical bonding, and dielectric properties. By maintaining identical material compositions and controlled parameters, the work establishes a clear structure-property relationship between fabrication approach and composite performance. The findings highlight the practical importance of the nonsolvent route as a cleaner and scalable option for producing flexible dielectric substrates suitable for RF and microwave applications.

To evaluate the structure-property relationships, comprehensive characterizations were conducted, including Fourier transform infrared spectroscopy (FTIR) to investigate chemical bonding and filler-matrix interfacial interactions and scanning electron microscopy (SEM) coupled with energy-dispersive X-ray spectroscopy (EDX) for assessing surface morphology and elemental distribution and dielectric behaviour (from 1 GHz to 10 GHz). These findings provide valuable insights into the effects of the fabrication method on composite quality and functionality, with direct implications for optimizing flexible dielectric substrates in RF and microwave applications.

2. Method

2.1. Material

Calcium copper titanate was purchased from Nanografi Nano Technology. The PDMS and elastomer curing agent (Slygard 184) were purchased from Dow Corning, USA. Ethanol was used in the lab. All the chemical reagents were used directly without purification.

2.2. Sample preparation via the solvent method

To prepare the CCTO/PDMS composite via the solvent method, CCTO and PDMS were first weighed to achieve composite loadings of 10 wt.%, 20 wt.%, 40 wt.%, and 60 wt.% by weight. Ethanol was then added to the mixture, which was subsequently sonicated for 20 minutes to promote uniform dispersion of the CCTO particles. After sonication, PDMS was added to the solution, followed by the addition of a stirring pill, and the mixture was placed on a magnetic hot plate and stirred at 85 °C at a stirring speed of 2 until the ethanol solvent completely evaporated. Once the solvent was fully removed, a curing agent with a ratio of 10:1 was added to the mixture and thoroughly blended. The composite was then poured into a mold and allowed to cure at room temperature for 48 hours to achieve full crosslinking and solidification.

2.3. Sample preparation via the non-solvent method

The CCTO/PDMS composites were prepared using a nonsolvent technique to obtain uniform ceramic dispersion and consistent dielectric response. Polydimethylsiloxane (PDMS, Sylgard 184, Dow Corning) and its curing agent were first mixed at a 10:1 weight ratio using an overhead mechanical stirrer at 2000 rpm for 10 min to form a homogeneous base matrix. Subsequently, CCTO powder was introduced into the PDMS mixture at various loadings (10, 20, 40, and 60 wt.%), followed by additional stirring at 2000 rpm for another 10 min to ensure even distribution of particles. CCTO/PDMS mixtures were then poured into a mold and left to cure naturally at room temperature (≈25 °C) for 24 h. Owing to the inherent fluidity and self-healing nature of the PDMS matrix, no degassing process was required to eliminate trapped air during curing.

2.4. Characterization

The morphologies of the CCTO/PDMS composites with concentrations of 10 wt.%, 20 wt.%, 40 wt.% and 60 wt.% were characterized via field emission scanning microscopy (FE-SEM, HITACHI S-4700) equipped with energy-dispersive X-ray spectroscopy (EDX). This combined technique enabled detailed visualization of the composite structure and precise mapping of their elemental compositions. The dielectric properties were measured at room temperature via a dielectric probe connected to a vector network analyser.

This setup allowed broadband measurement of the real and imaginary parts of the permittivity, providing insight into the frequency-dependent dielectric behaviour of the composites. Each dielectric measurement was repeated four times, and the average values were reported to ensure reproducibility. Fourier transform infrared spectroscopy (FTIR) analysis was performed using a Nicolet iS50 FT-IR

spectrometer to investigate the chemical bonding and functional groups present in the composites. The spectra were recorded in the range of 400–4000 cm^{-1} to identify characteristic absorption peaks corresponding to both the polymer matrix and ceramic filler.

3. Result and Discussion

3.1. Surface morphology and composition analysis

Figure 1 shows the SEM image of CCCTO-PDMS prepared via the nonsolvent method, with filler loadings of 10, 20, 40, and 60 wt.%. At 10 wt.% (Fig. 1(a)), the surface appears relatively smooth with limited particle visibility, indicating good polymer continuity and low filler agglomeration. Increasing the filler to 20 wt.% (Fig. 1(b)) results in a greater number of exposed CCTO particles, with some evidence of interfacial voids and filler pull-outs, likely due to weaker filler-matrix bonding. A more dramatic morphological shift is observed at 40 wt.% (Fig. 1(c)), where the surface becomes rougher and irregular, with numerous CCTO clusters forming along the fractured surface. At 60 wt.% (Fig. 1(d)), the morphology indicates extensive filler coverage with reduced polymer phase visibility, suggesting the onset of particle crowding and partial filler–filler connectivity, which can contribute to increased dielectric pathways.

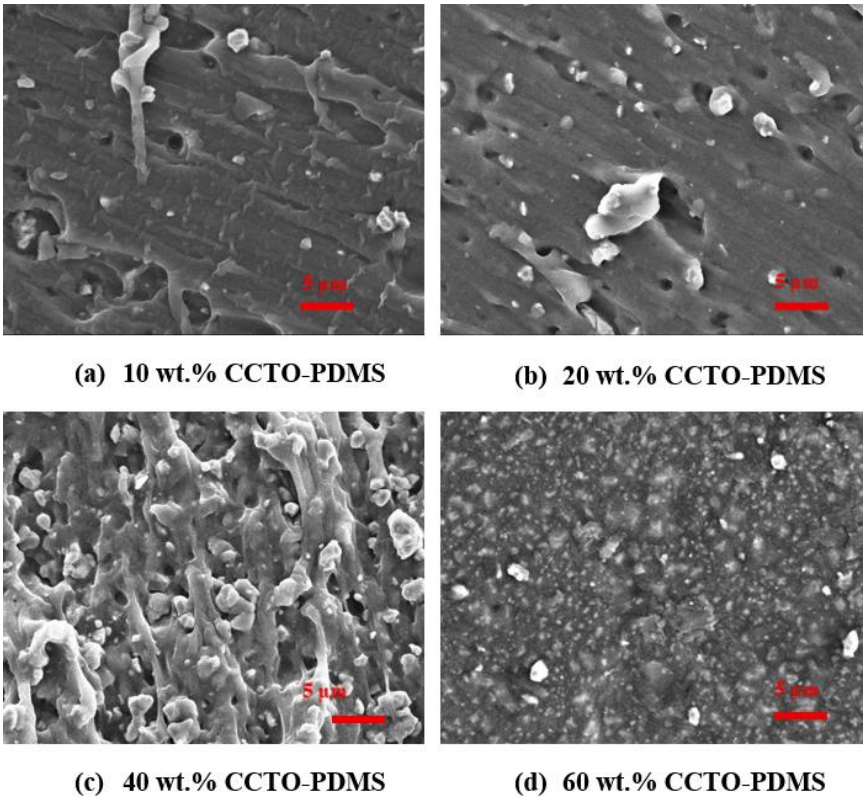

(a) 10 wt.% CCTO-PDMS **(b) 20 wt.% CCTO-PDMS**

(c) 40 wt.% CCTO-PDMS **(d) 60 wt.% CCTO-PDMS**

Fig. 1. SEM micrographs of CCTO-PDMS composites fabricated via the nonsolvent method with varying CCTO loadings: (a) 10 wt.%, (b) 20 wt.%, (c) 40 wt.%, and (d) 60 wt.%.

In contrast, Fig. 2 shows the SEM image of CCTO-PDMS prepared via the solvent method, which provides lower magnification SEM images that emphasize the particle distribution across a wider surface area. At 10 wt.% and 20 wt.% (Figs. 2(a) and 2(b)), the micrographs show sparsely scattered and isolated CCTO particles with minimal agglomeration, indicating effective dispersion at lower concentrations. As the loading increases to 40 wt.% and 60 wt.% (Figs. 2(c) and 2(d)), the surface becomes more populated with fine CCTO particles that are more evenly distributed, although some overlap and clustering are visible at the highest concentration. The more homogeneous distribution in these wider-area scans suggests that, while microroughness is pronounced in the fractured cross section (Fig. 1), the bulk surface remains relatively uniform, especially at higher filler contents. This finding supports the inference that the nonsolvent method promotes consistent filler dispersion, even at higher loadings, due to the absence of solvent-induced phase separation or drying stresses.

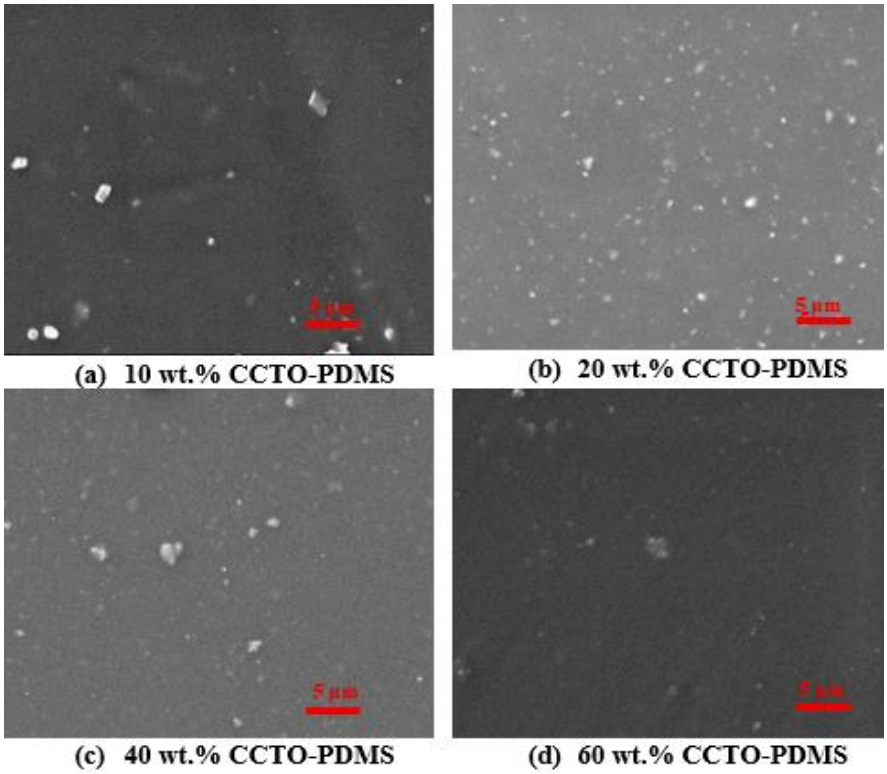

Fig. 2. SEM micrographs of CCTO-PDMS composites prepared via the solvent method with varying CCTO loadings: (a) 10 wt.%, (b) 20 wt.%, (c) 40 wt.%, and (d) 60 wt.%.

When Figs. 1 and 2 are compared, a clear correlation can be observed between increasing filler loading and the transition from a matrix-dominated morphology to one increasingly influenced by filler interactions. The microstructural features observed at 40 wt.% and especially at 60 wt.% suggest that the composite is approaching or exceeding this percolation threshold. Moreover, the gradual increase in interfacial areas observed aligns with the Maxwell-Wagner-Sillars

(MWS) polarization theory, which predicts enhanced interfacial charge accumulation in heterogeneous systems comprising high-permittivity fillers embedded in low-permittivity matrices [3].

3.2. FTIR analysis of chemical bonding and interfacial interactions

Figure 3 shows the FTIR spectrum of CCTO-PDMS prepared via the nonsolvent method, confirming the chemical integrity of both the PDMS and CCTO phases within the composite. The strong band at 2959.76 cm^{-1} corresponds to Si–CH_3 symmetric stretching, whereas the band at 1259.79 cm^{-1} is attributed to CH_3 bending in Si–CH_3, indicating that the PDMS methyl side groups remain intact after composite processing. The peaks at 1089.12 cm^{-1} and 1023.07 cm^{-1} represent Si–O–Si stretching vibrations, confirming the preservation of the siloxane backbone without chemical cross-linking or degradation. Minor bands at 861.67 cm^{-1} and 800.81 cm^{-1} arise from C–H bending and CH_3 rocking, respectively. Critically, the peak at 564.47 cm^{-1}, which increases with filler content, is assigned to M–O stretching (M = Ti, Cu) in the TiO_6 and CuO_4 units of the CCTO lattice. This indicates successful physical dispersion of the CCTO particles within the matrix. The absence of new functional groups or band shifts suggests that no covalent interaction occurs between PDMS and CCTO, preserving the intrinsic dielectric nature of each phase. These results are consistent with the literature on the use of PDMS-ceramic composites for flexible dielectric applications [25, 26].

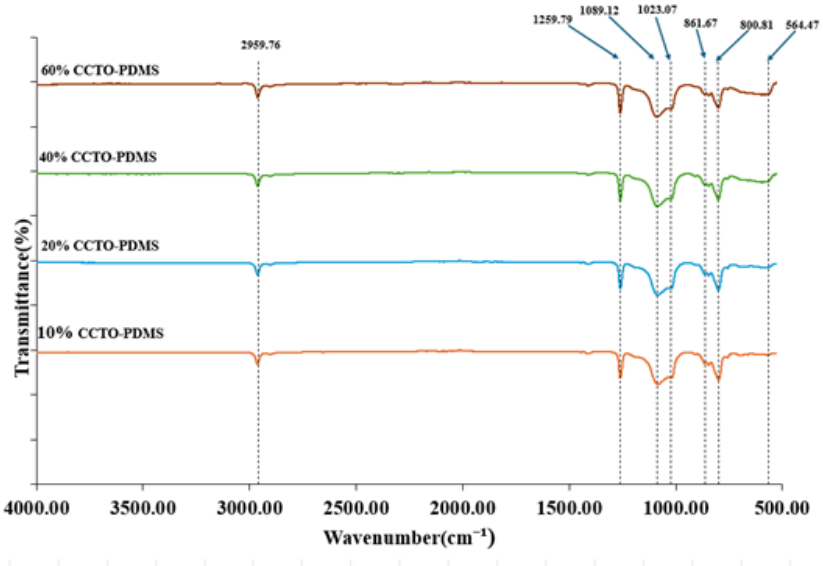

Fig. 1. FTIR characterization of the CCTO-PDMS composite prepared without solvent.

Figure 4 presents the FTIR spectra of the CCTO-PDMS composites prepared via the solvent method, revealing characteristic vibrations of both the PDMS and the ceramic filler. The peak at 2962.17 cm^{-1} corresponds to the symmetric stretching of CH_3 groups, whereas the peak at 1260.75 cm^{-1} is assigned to the bending of Si-CH_3, both confirming the preservation of the PDMS side groups [25].

The Si-O-Si asymmetric and symmetric stretching modes appear at 1086.23 cm^{-1} and 1014.87 cm^{-1}, respectively, which is consistent with the siloxane backbone [26]. The 799.84 cm^{-1} band corresponds to rocking vibrations of Si-$(CH_3)_2$ units [25]. Importantly, the peak at 558.30 cm^{-1} clearly increases in intensity with increasing filler content, which is attributed to M-O stretching vibrations (Ti-O, Cu-O) in the CCTO lattice [26, 27]. The absence of new peaks or spectral shifts suggests that no covalent interaction occurs between the matrix and filler, indicating a physically dispersed two-phase system which is consistent with previous CCTO-PDMS studies [10].

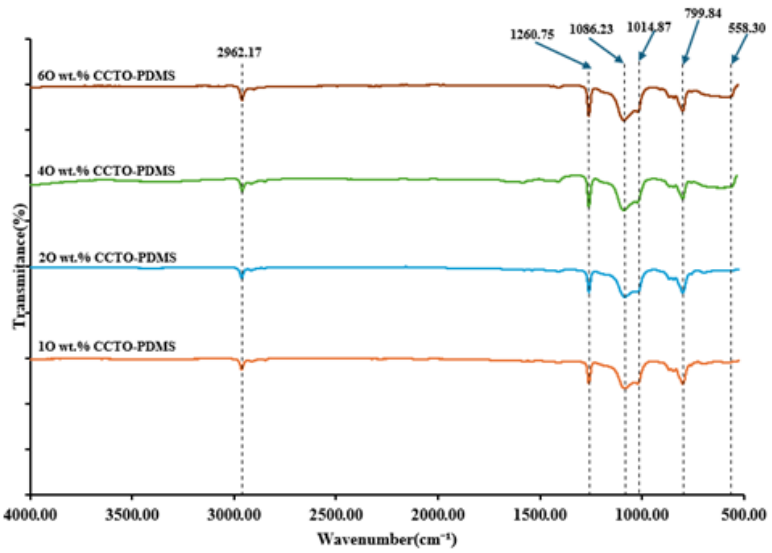

Fig. 2. FTIR characterization of the CCTO-PDMS composite prepared with solvent.

3.3. Dielectric permittivity, loss tangent, and AC conductivity analysis

Figure 5 shows the real and imaginary parts of the permittivity for the CCTO-PDMS composites fabricated via the solvent and nonsolvent methods at various CCTO filler loadings (10-60 wt.%). As expected, the dielectric constant slightly decreases with increasing frequency for all the samples. This behaviour is typical due to the inability of dipoles to respond quickly at higher frequencies. he nonsolvent 60% composite exhibited the highest dielectric constant across the measured frequency range, with a value of 5.49 at 5.2 GHz.

This is followed closely by the addition of 60% solvent, which reaches 5.05 at the same frequency. The high dielectric values in these samples are likely due to the higher content of CCTO, which contributes to stronger interfacial polarization. In contrast, samples with 10% CCTO, especially those prepared via the solvent method, typically have much lower dielectric constants (below 3.0). These findings suggest that both the filler content and the fabrication method significantly influence the dielectric behaviour of the composites. Nonsolvent samples consistently show higher permittivity than solvent-based samples do, possibly due to differences in dispersion and interface structure.

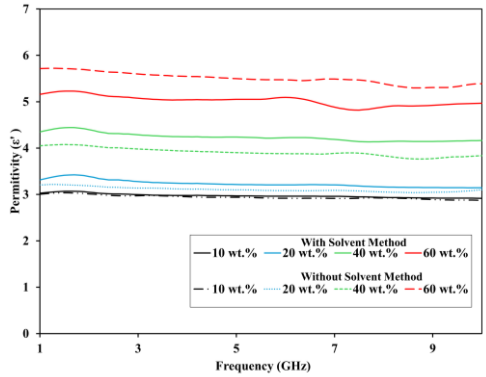

(a) Real part of the permittivity (ε′).

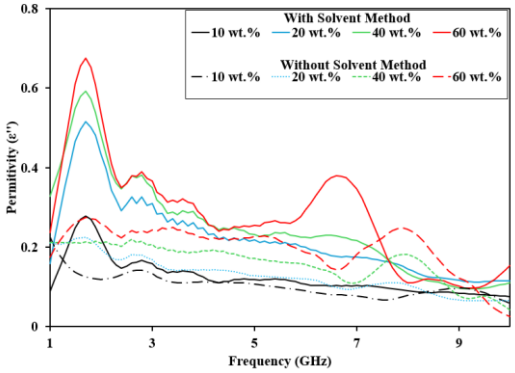

(b) imaginary part of the permittivity (ε″).

Fig. 3. (a) Real part of the permittivity (ε′) and (b) imaginary part of the permittivity (ε″) as a function of frequency (1–10 GHz) for CCTO-PDMS composites fabricated via the solvent and nonsolvent methods at various CCTO filler loadings (10–60 wt.%).

Figure 6 shows the tangent loss graph for a range of frequencies for both the solvent and nonsolvent samples with different CCTO loadings. In general, the tangent loss decreases as the frequency increases for all the samples. This trend is expected because energy losses tend to decrease at higher frequencies because of less interfacial polarization. At 5.2 GHz, the lowest loss is observed in the nonsolvent 10% sample, with a value of 0.035. This indicates minimal energy loss during signal transmission, which is ideal for high-frequency applications.

On the other hand, the highest loss among the solvent samples occurred for the 20% and 40% composite samples, with values of 0.067 and 0.055, respectively. Interestingly, despite having high dielectric constants, the nonsolvent 60% and solvent 60% samples maintained moderate losses at 0.042 and 0.052, respectively. These results highlight the trade-off between achieving a high dielectric constant and maintaining low energy dissipation. While a higher filler content improves the permittivity, it may also increase the chance of particle clustering or interface defects, which can contribute to energy loss.

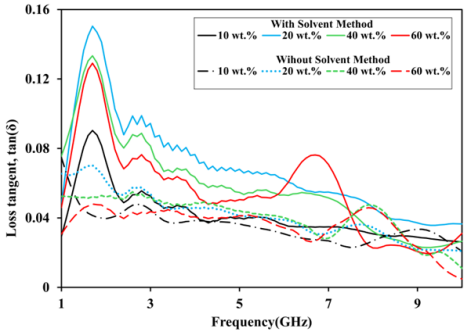

Fig. 4. Comparison of the dielectric loss tangent (tan δ) of CCTO-PDMS composites fabricated via the solvent and nonsolvent methods at varying filler loadings (10-60 wt.%) over the 1-10 GHz frequency range.

The electrical conductivity behaviour of the CCTO-PDMS composites, as illustrated in Fig. 7, clearly depends on both the filler loading and the fabrication method across the 1–10 GHz frequency range. A clear trend is observed where the conductivity increases with increasing CCTO content for both fabrication approaches. However, the solvent-assisted composites consistently exhibit higher conductivity values than their nonsolvent counterparts do, particularly at higher loadings. This enhancement is attributed to more homogeneous particle dispersion and stronger interfacial contact achieved through the solvent-mediated mixing process, which facilitates the formation of continuous conductive pathways within the PDMS matrix [28].

The most significant improvement in electrical conductivity was observed for the 60 wt.% solvent-based composite, which reached a peak value of approximately 0.15 S/m near 7.5 GHz. This indicates the formation of a well-connected percolation network, enabling effective charge transport under high-frequency excitation. According to classical percolation theory, once the volume fraction exceeds the percolation threshold, the conductivity follows a power law with increasing filler concentration [29]. This critical behaviour also impacts the dielectric constant, which can rise sharply near the threshold due to enhanced interfacial and dipolar polarization [30].

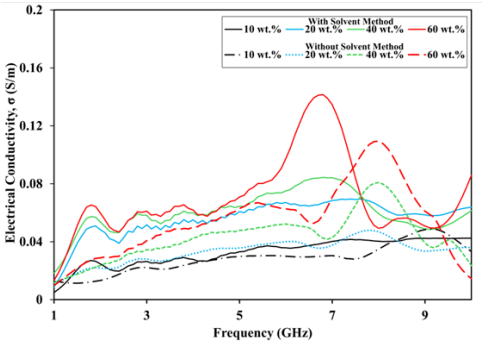

Fig. 5. Electrical conductivity of CCTO-PDMS composites with different filler loadings (10-60 wt.%) obtained via the solvent and nonsolvent methods from 1-10 GHz.

4. Discussion of the Results

The dielectric performance of the CCTO-PDMS composites prepared via the solvent and nonsolvent methods is illustrated in Figs. 8 and 9. These figures show the variation in real (ε') and imaginary (ε'') permittivity, as well as the loss tangent (tan δ), as a function of ceramic filler loading from 10 to 60 wt.%. The real permittivity (ε') consistently increases with increasing filler content for both fabrication methods, reflecting the dominant contribution of the high dielectric constant of CCTO. Notably, at 60 wt.%, the composite fabricated without solvent exhibited a higher ε' than did the solvent-based method.

This suggests that the nonsolvent route may facilitate better particle connectivity or denser packing, which enhances interfacial polarization, a mechanism aligned with the Maxwell–Wagner–Sillars (MWS) theory for heterogeneous dielectric systems [31]. The imaginary permittivity (ε'') also increases with filler content, albeit at a much lower scale, which is typical of systems where dielectric losses are primarily capacitive. However, the nonsolvent sample still has a slightly lower ε'' across the range, especially at 60 wt.%, suggesting lower energy dissipation.

The loss tangent (tan δ), which represents the dielectric loss, peaks at moderate loading for the solvent-based composite but decreases beyond 30 wt.%. In contrast, the nonsolvent method results in relatively stable and lower tan δ values across the loading range. At 60 wt.%, the nonsolvent composite achieves both a higher ε' and a lower tan δ, indicating that it is a superior performer in terms of balancing dielectric enhancement with minimal losses. These results indicate that the nonsolvent method results in a more stable dielectric system, potentially due to reduced filler aggregation and better interfacial compatibility. This behaviour aligns with percolation theory, where filler distribution and network formation critically influence dielectric behaviour without severely compromising insulation properties [32].

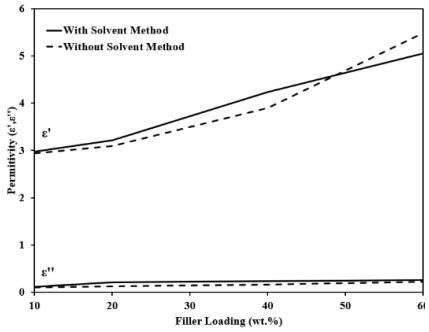

Fig. 8. Real and imaginary permittivity vs. filler loading in CCTO-PDMS composites prepared by solvent and non-solvent methods.

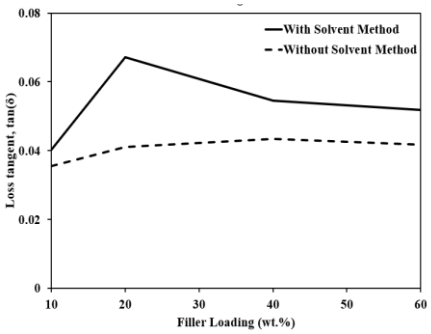

Fig. 9. Loss tangent vs. filler loading for CCTO-PDMS composites prepared by solvent and non-solvent methods.

Figure 10 shows the variation in electrical conductivity (σ) of the CCTO–PDMS composites with increasing filler loading, comparing samples fabricated via the solvent and nonsolvent methods. The conductivity is observed to increase for both

methods as the CCTO content increases from 10 to 60 wt.%, which is consistent with the well-established percolation theory. As the ceramic filler concentration approaches the percolation threshold, the probability of forming continuous conductive paths within the insulating polymer matrix increases significantly [33]. At low filler concentrations (10–20 wt.%), both methods result in a gradual increase in conductivity. However, the composite prepared via the solvent-based method displays a steeper increase, especially between 10 and 20 wt.%, suggesting earlier percolation onset or better filler connectivity due to enhanced dispersion during solvent-assisted mixing.

Beyond 30 wt.%, conductivity plateaus for the solvent-based samples, indicating that most percolative paths have already been established. In contrast, the non-solvent method results in a steady and linear increase in conductivity with increasing filler loading. At 60 wt.%, the nonsolvent sample nearly matches the conductivity level of the solvent-based composite, despite initially lagging at lower filler contents. This convergence in performance at higher loadings highlights the nonsolvent method's ability to support percolative network formation without the need for solvent dispersion, possibly due to improved interfacial packing and reduced agglomeration. Importantly, this conductivity improvement is achieved without a dramatic increase in dielectric loss, as seen in the earlier loss tangent data (Fig. 9), positioning the nonsolvent approach as a promising route for applications requiring both high permittivity and moderate conductivity.

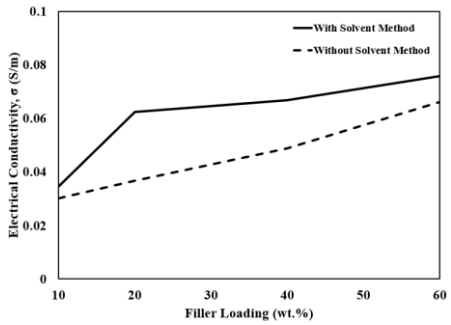

Fig. 10. Electrical conductivity vs. filler loading for CCTO-PDMS composites prepared via solvent and non-solvent methods.

A comparative analysis of CCTO-PDMS composites fabricated via solvent and nonsolvent methods revealed that filler loading significantly influences the dielectric and electrical properties. Across all three plots, the nonsolvent method consistently demonstrated superior performance at 60 wt.%, achieving the highest real permittivity with a lower loss tangent and maintaining electrical conductivity comparable to that of its solvent-based counterpart.

This suggests that the nonsolvent approach promotes better filler packing and interfacial polarization while minimizing dielectric losses, making it more effective for applications requiring high dielectric constants with stable energy dissipation. Moreover, the steady conductivity trend implies a more uniform filler distribution without excessive aggregation. These findings indicate that the nonsolvent method offers a more reliable route for engineering flexible dielectric composites with balanced electrical characteristics. Comparison of the Dielectric Properties of

CCTO–PDMS Composites at 5.2 GHz via Solvent and Non-Solvent Methods at a filler loading of 60 wt.% CCTO as shown in Table 1.

Table 1. Comparison of the Dielectric Properties of CCTO-PDMS Composites at 5.2 GHz via Solvent and Non-Solvent Methods at a filler loading of 60 wt.% CCTO.

	Solvent method	Non-solvent method
Dielectric constant (ε')	5.051766	5.488778
Tangent loss (tan(δ))	0.051874	0.041679
Conductivity σ (S/m)	0.075804	0.066154

As summarized in Table 2, the dielectric performance of CCTO-based polymer composites reported in previous studies varies considerably with polymer type and testing frequency. Composites incorporating highly polar matrices such as TPU and PVDF exhibited notably higher dielectric constants, reaching 56.00 at 1 kHz [38] and 20.00 [37], respectively, due to their strong dipolar polarization and higher ceramic–polymer interfacial interaction. In contrast, systems based on less polar matrices, including PTFE (εr = 12.67 at 8.84 GHz) [35] and PPO (εr = 7.08) [36], displayed moderate dielectric responses. The present CCTO–PDMS composite demonstrates dielectric permittivity values of 6.01 at 1.1 GHz and 5.48 at 5.2 GHz, indicating stable dielectric behaviour in the microwave region. Although the εr values are slightly lower compared to other polymer systems, PDMS provides superior mechanical flexibility and environmental stability, essential for wearable and flexible antenna applications. Therefore, the obtained results confirm that the CCTO–PDMS composite offers a balanced combination of dielectric performance and flexibility suitable for high-frequency substrate design.

Table 1. Comparative summary of dielectric permittivity values for CCTO-based polymer composites reported in the present work.

Composite Material	Measurement Frequency	Dielectric Permittivity (εr)	Ref.
CCTO 60 wt.% + PDMS	5.2 GHz	5.48	This work
CCTO 60 wt.% + PDMS	1.1 GHz	6.01	This work
CCTO 20 wt.% + PDMS	50 Hz	4.37 – 4.18	[34]
CCTO 50 wt.% + PTFE	8.84 GHz	12.67	[35]
CCTO 30 wt.% + PPO	Not specified	7.08	[36]
CCTO-NFs (20%) + PVDF	Not specified	20.00	[37]
CCTO 40 wt.% + TPU	1 kHz	56.00	[38]

5. Conclusion

The comparative results show that the nonsolvent fabrication route provides better dielectric performance in CCTO–PDMS composites, particularly at higher filler loadings. At 60 wt.%, the nonsolvent sample demonstrated higher real permittivity, lower dielectric loss, and more stable conductivity, attributed to improved filler

dispersion and stronger interfacial packing. The absence of solvent minimized drying-induced voids or phase separation, resulting in a more homogeneous microstructure and enhanced dielectric uniformity. However, one inherent limitation of PDMS lies in its intrinsically low polarity and weak interfacial polarization compared to more polar polymers such as PVDF or TPU, which restricts its achievable dielectric constant even at high ceramic loadings.

This drawback arises from the low dielectric nature of the PDMS backbone, where limited dipolar orientation contributes to reduced overall permittivity. Future work should focus on surface functionalization of CCTO particles, chemical modification of PDMS chains, or hybrid blending with moderately polar polymers to improve interfacial polarization and dielectric enhancement while retaining mechanical flexibility. These strategies could further optimize CCTO–PDMS composites for next-generation high-frequency and flexible electronic applications.

Future studies should focus on further optimization of CCTO–PDMS composites to enhance both their dielectric and mechanical characteristics for flexible antenna applications. Several approaches may be therefore explored, including surface functionalization of CCTO nanoparticles to improve interfacial compatibility with the PDMS matrix and reduce agglomeration at higher filler loadings. Chemical modification or copolymerization of PDMS with moderately polar polymers could also increase interfacial polarization without sacrificing elasticity.

In addition, future investigations should evaluate the bending reliability, thermal stability, and long-term electrical endurance of the composites under dynamic deformation to simulate real wearable conditions. From a device perspective, integrating the optimized composites into microstrip or conformal antenna prototypes will provide valuable insight into their impedance matching, bandwidth stability, and radiation performance under mechanical strain. Such studies would strengthen the understanding of structure–property relationships and support the development of next-generation flexible microwave systems.

Acknowledgement

This work has been supported by the Ministry of Higher Education Malaysia (MoHE) FRGS grant FRGS/1/2024/TK09/UMP/03/1 (RDU240105) and Universiti Malaysia Pahang Al-Sultan Abdullah (UMPSA). Their involvement enabled the successful completion of our research at the UMPSA STEM Lab, the Faculty of Electrical and Electronics Engineering Technology, UMPSA.

Reference

1. Ananthakrishnan, A.T. (2008). Flexible circuits market: Surging ahead. *SMT Surface Mount Technology*, 22(3), 14-16.
2. Gamota, D. (2009). Near-term opportunities for large-area flexible electronics. *Printed Circuit Design & Manufacture*, 26(4), 27-29.
3. Haji Omer, H.A.; Azemi, S.N.; Al-Hadi, A.A.; Soh, P.J.; and Jamlos, M.F. (2018). Structural health monitoring sensor based on a flexible microstrip patch antenna. *Indonesian Journal of Electrical Engineering and Computer Science*, 10(3), 917-924.

4. Salleh, S.M.; Ain, M.F.; Ahmad, Z.; Abidin, I.S.Z.; Seng, L.Y.; and Osman, M.N. (2023). Stretchable and bendable polydimethylsiloxane-silver composite antenna on PDMS/air gap substrate for 5G wearable applications. *IEEE Access*, 11, 133623-133639.
5. Sharma, A.; and Kumar, P. (2022). Design of a flexible microstrip antenna for BAN Applications. *Journal of Physics*: *Conference Series*, 2161(1), 012012.
6. Xu, X.; Liu, W.; Li, Y.; Wang, Y.; Yuan, Q.; Chen, J.; Ma, R.; Xiang, F.; and Wang, H. (2018). Flexible mica films for high-temperature energy storage. *Journal of Materiomics*, 4(3), 173-178.
7. Cui, Y.; Wang, X.; Chi, Q.G.; Dong, J.F.; Ma, T.; and Lei, Q.Q. (2017). Improving dielectric properties of PVDF composites by obtaining the BT-Ni particles. *Proceedings of the* 2017 1st *International Conference on Electrical Materials and Power Equipment* (*ICEMPE*), Xi'an, China, 239-243.
8. Xu, F.; Yang, Y.; Liu, Y.; Yang, J.; Liao, Y.; Wang, X.; Shi, X.; and Hu, J. (2021). Ferrite ceramic filled poly-dimethylsiloxane composite with enhanced magnetic-dielectric properties as substrate material for flexible electronics. *Ceramics International*, 47(13), 18246-18251.
9. Rajitha, G.; and Dash, R.K. (2018). Optically transparent and high dielectric constant reduced graphene oxide (RGO)-PDMS based flexible composite for wearable and flexible sensors. *Sensors and Actuators A*: *Physical*, 277, 26-34.
10. Wang, W.; Ren, G.; Zhou, M.; and Deng, W. (2021). Preparation and characterization of CCTO/PDMS dielectric elastomers with high dielectric constant and low dielectric loss. *Polymers*, 13(7), 1075.
11. Romasanta, L.J.; Leret, P.; Casaban, L.; Hernández, M.; De La Rubia, M.A.; Fernández, J.F.; Kenny, J.M.; Lopez-Manchado, M.A.; and Verdejo, R. (2012). Towards materials with enhanced electro-mechanical response: $CaCu_3Ti_4O_{12}$-polydimethylsiloxane composites. *Journal of Materials Chemistry*, 22(47), 24705-24712.
12. Liu, G.; Chen, Y.; Gong, M.; Liu, X.; Cui, Z.K.; Pei, Q.; Gu, J.; Huang, C.; and Zhuang, Q. (2018). Enhanced dielectric performance of PDMS-based three-phase percolative nanocomposite films incorporating a high dielectric constant ceramic and conductive multi-walled carbon nanotubes. *Journal of Materials Chemistry C*, 6(40),10829-10837.
13. Liu, Y.; Wu, P.; Kang, P.; Li, L.; Shi, J.; Zhou, Z.; Chen, G.-X.; Li, Q. (2021). PDMS-based composites with stable dielectric properties at varied frequency via Sr-doped $CaCu_3Ti_4O_{12}$ nanowires for flexible wideband antenna substrate. *Journal of Materials Science*: *Materials in Electronics*, 32(1), 430-441.
14. Zhang, L.; Song, F.; Lin, X.; and Wang, D. (2020). High-dielectric-permittivity silicone rubbers incorporated with polydopamine-modified ceramics and their potential application as dielectric elastomer generator. *Materials Chemistry and Physics*, 241, 122373.
15. Mu, C.; Li, J.; Song, Y.; Huang, W.; Ran, A.; Deng, K.; Huang, J.; Xie, W.; Sun, R.; and Zhang, H. (2018). Enhanced piezocapacitive effect in $CaCu_3Ti_4O_{12}$-polydimethylsiloxane composited sponge for ultrasensitive flexible capacitive sensor. *ACS Applied Nano Materials*, 1(1), 274-283.

16. Tang, X.; Gu, Q.; Gao, P.; and Wen, W. (2021). Ultra-sensitive wide-range small capacitive pressure sensor based on porous CCTO-PDMS membrane. *Sensors and Actuators Reports*, 3, 100027.
17. Azani, M.-R.; and Hassanpour, A. (2024). Nanotechnology in the fabrication of advanced paints and coatings: Dispersion and stabilization mechanisms for enhanced performance. *ChemistrySelect*, 9(19), e202400844.
18. Sattar, R.; Kausar, A.; and Siddiq, M. (2015). Advances in thermoplastic polyurethane composites reinforced with carbon nanotubes and carbon nanofibers: A review. *Journal of Plastic Film & Sheeting,* 31(2), 186-224.
19. Ha, H.; Mueller, S.; Guriyanova, S.; and Hwang, B. (2025). Surface energy characterization of a single microsphere particle using peakforce quantitative nanomechanical mapping mode of atomic force microscope. *Facta Universitatis, Series*: *Mechanical Engineering*, 23(1), 171-181.
20. Sharifuddin, S.M.; Nor, M.S.M.; Pabli, F.A.M.; Chueangchayaphan, W.; Ahmad, Z.A.; and Sulaiman, M.A. (2022). Modification of curing, morphological, mechanical and electrical properties of epoxidised natural rubber (ENR-25) through the addition of copper calcium titanium oxide (CCTO). *Polymer Bulletin*, 79(11), 9907-9923.
21. Zhao, D.; Liu, W.; Chen, J.; Yue, G.; Song, Q.; and Yang, Y. (2024). Interlaminar bonding of high-performance thermoplastic composites during automated fiber placement in-situ consolidation. *Journal of Composite Materials*, 58(20), 2247-2261.
22. Rosseto, M.P.; Lenzi, E.K.; Pedrozo Da Silva, A.C.; Tessaro, A.L.; Ribeiro De Almeida, R.R.; Evangelista, L.R.; and Zola, R.S. (2025). Investigating solvents dielectric response with impedance spectroscopy and an extend Poisson-Nernst-Planck (PNP) model. *Journal of Molecular Liquids*, 423, 127184.
23. Dutkiewicz, M.; and Dutkiewicz, E. (2006). Study of microheterogeneous structure of non-aqueous mixed solvents by non-linear dielectric and viscometric methods. *Electrochim Acta*, 51(11), 2346-2350.
24. Kahrs, C.; and Schwellenbach, J. (2020). Membrane formation via non-solvent induced phase separation using sustainable solvents: A comparative study. *Polymer*, 186, 122071.
25. Vazirinasab, E. (2020). *Superhydrophobic silicone-based nanocomposites for application to high voltage insulator*. PhD Thesis, Department of Applied Sciences, Université du Québec à Chicoutimi.
26. Hadi, N.; Abdi, F.; Lamcharfi, T.; Belaaraj, A.; Kassou, S.; and Ahjyaje, F. (2019). Study of the dielectric, optical and microstructure properties of $CaCu_3Ti_4O_{12}$-$PbZr_{0.48}Ti_{0.52}O_3$ ceramic system with different compositions. *Mediterranean Journal of Chemistry*, 8(3), 245.
27. Jesurani, S.; Kanagesan, S.; Velmurugan, R.; and Kalaivani, T. (2012). Phase formation and high dielectric constant of calcium copper titanate using sol-gel route. *Journal of Materials Science*: *Materials in Electronics*, 23(3), 668-674.
28. Dang, Z.-M.; Yuan, J.-K.; Zha, J.-W.; Zhou, T.; Li, S.-T.; and Hu, G.-H. (2012). Fundamentals, processes and applications of high-permittivity polymer–matrix composites. *Progress in Materials Science*, 57(4), 660-723.
29. Rahaman, M.; Aldalbahi, A.; Govindasami, P.; Khanam, N.; Bhandari, S.; Feng, P.; and Altalhi, T. (2017). A new insight in determining the percolation

threshold of electrical conductivity for extrinsically conducting polymer composites through different sigmoidal models. *Polymers*, 9(10), 527.

30. Nan, C.-W.; Shen, Y.; and Ma, J. (2010). Physical properties of composites near percolation. *Annual Review of Materials Research*, 40(1), 131-151.
31. Samet, M.; Boiteux, G.; Seytre, G.; Kallel, A.; and Serghei, A. (2014). Interfacial polarization in composite materials with spherical fillers: Characteristic frequencies and scaling laws. *Colloid and Polymer Science*, 292(8), 1977-1988.
32. Dang, Z.-M.; Yuan, J.-K.; Yao, S.-H.; and Liao, R.-J. (2013). Flexible nanodielectric materials with high permittivity for power energy storage. *Advanced Materials*, 25(44), 6334-6365.
33. Grimaldi, C.; and Balberg, I. (2006). Tunneling and nonuniversality in continuum percolation systems. *Physical Review Letters*, 96, 066602.
34. Wang, G.L.; Zhang, Y.Y.; Duan, L.; Ding, K.H.; Wang, Z.F.; and Zhang, M. (2015). Property reinforcement of silicone dielectric elastomers filled with self-prepared calcium copper titanate particles. *Journal of Applied Polymer Science*, 132(39), app.42613.
35. Liang, F.; Zhao, Y.; Chen, X.; Wan, Q.; and Lü, W. (2019). Dielectric properties of Polytetrafluoroethylene/$CaCu_3Ti_4O_{12}$ composites. *Journal of Wuhan University of Technology-Mater. Sci. Ed.*, 34(1), 189-194.
36. Wang, S.; He, X.; Chen, Q.; Chen, Y.; He, W.; Zhou, G.; Zhang, H.; Jin, X.; and Su, X. (2018). Graphene-coated copper calcium titanate to improve dielectric performance of PPO-based composite. *Materials Letters*, 233, 355-358.
37. Hu, C.-H.; Zha, J.-W.; Yang, Y.; Zheng, M.-S.; and Dang, Z.-M. (2017). Enhanced dielectric properties of polyvinylidene fluoride nanocomposites via calcium copper titanate nanofibers. *Proceedings of the* 2017 1st *International Conference on Electrical Materials and Power Equipment* (*ICEMPE*), Xi'an, China, 258-261.
38. Variar, L.; Muralidharan, M.N.; Narayanankutty, S.K.; and Ansari, S. (2021). High dielectric constant, flexible and easy-processable calcium copper titanate/thermoplastic polyurethane (CCTO/TPU) composites through simple casting method. *Journal of Materials Science*: *Materials in Electronics*, 32(5), 5908-5919.